Co-operative interactions of oligonucleosomal DNA with the H1e histone variant and its poly(ADP-ribosyl)ated isoform

Maria D'ERME*, Giuseppe ZARDO†, Anna REALE‡ and Paola CAIAFA†§

*Dipartimento di Scienze Biochimiche, 'A. Rossi Fanelli' Università di Roma 'La Sapienza', Piazzale A. Moro 5, I-00185, Roma,
†Dipartimento di Scienze e Tecnologie Biomediche e di Biometria, Università degli Studi dell'Aquila, via Vetoio, I-67100 Coppito, L'Aquila, Italy, and
‡Dipartimento di Biopatologia, Umana Università di Roma 'La Sapienza', Viale Regina Elena 324, I-00161, Roma, Italy

H1 histone somatic variants from L929 mouse fibroblasts were purified by reverse-phase HPLC. We analysed the ability of each H1 histone variant to allow the H1–H1 interactions that are essential for the formation of the higher levels of chromatin structure, and we investigated the role played by the poly(ADP-ribosyl)ation process. Cross-linking analysis showed that H1e is the only somatic variant which, when bound to DNA, is able to produce H1–H1 polymers; the size of polymers was decreased when H1e was enriched in its poly(ADP-ribosyl)ated isoform. Measurement of the methyl-accepting ability in native nuclei compared with nuclei in which poly(ADP-ribosyl)ation was induced showed that the poly(ADP-ribosyl)ated H1 histone had not been removed from linker regions, in spite of its different interaction with DNA.

INTRODUCTION

In eukaryotic cells histone H1 organizes the polynucleosome chain into higher-order chromatin structure [1–3], with each of the three domains of this histone playing a specific role in chromatin condensation. The globular region of histone H1 closes the structure of the 'core' particle by its specific contacts with histone octamer via the C-terminal tail of histone H2a [4] and by sealing the DNA regions which enter and exit from the core particle [5,6]. The C-terminal region of histone H1 interacts with linker DNA, while the N-terminal region interacts with an unidentified core histone in neighbouring nucleosomes [7–9]. H1 is, moreover, implicated (although there is still much discussion as to where or how it is located at the second level of chromatin organization [10–13]) in the formation of the condensed fibre via H1–H1 interactions [1,2], which probably involve its N-terminal and globular domains [9]. At the third level of chromatin structure, H1 is present within the regions (scaffold attachment regions) where the chromatin loops are anchored to the nuclear scaffold [14].

There are, however, within the H1 histone family a number of somatic variants, the major ones being H1a, H1b, H1c, H1d and H1e (reviewed in [15]). They all have a three-domain structure, with a highly conserved central globular domain (98% identity in its 80-amino-acid sequence). The differences between the variants are localized in the N-terminal and C-terminal tails (which consist of about 40 and 100 amino acids respectively) [15], with the overall variation in molecular mass being approx. 1.0–1.4 kDa.

The numbers and relative amounts of these somatic variants are known to differ in condensed compared with decondensed chromatin, in various tissues and species, through the developmental stages of an organism, in dividing compared with non-dividing cells, and upon neoplastic transformation [15–26]. Some of these variants are implicated in important processes: H1e/H1c [27], and more precisely the H1e variant (G. Zardo, R. Santoro, M. D'Erme, A. Reale, L. Guidobaldi, P. Caiafa and R. Strom, unpublished work), regulate the mechanism of *in vitro* DNA methylation, while the H1c variant seems to inhibit the transcription process [28].

Some studies, carried out by utilizing different methodological approaches, propose for the H1 histone variants different efficiencies in promoting chromatin condensation [23–26]. It is often assumed [29–33] that the artificially reconstituted structure of DNA–H1 complexes formed under conditions of co-operative binding [30,32] mirrors the structure at H1 binding sites in chromatin. Two tissue-specific members of the H1 family, namely H5 from chicken erythrocytes and spH1 from sea urchin sperm, have shown co-operative binding to linear double-stranded DNA at low ionic strength (5 mM NaCl), while the binding of bulk H1 to DNA is co-operative only at NaCl concentrations of 35 mM and above [32].

In the present paper we have studied the efficiency of the different H1 histone somatic variants in forming cross-linking polymers when bound to DNA. The different efficiencies of the somatic variants in the formation of cross-links may have implications for the condensation of chromatin. A further complexity arises from the existence of post-synthetic modifications [33] which increase histone H1 heterogeneity and account for the numerous structural [1,5,14,30] and functional [27,34–39] roles played by this histone in chromatin.

Among the possible modifications of H1 histone, we have chosen to investigate its poly(ADP-ribosyl)ation, which appears to be closely correlated with some processes leading to chromatin relaxation [40–46]. This post-synthetic modification alters the chromatin structure by introducing a progressively larger number of negative charges in the C- and N-terminal tails, which are involved in the H1–H1 interactions essential for maintaining the three-dimensional structure of chromatin [1,2,7,47]. In order to understand the role of each variant in the formation of the higher-order chromatin structure and the possible regulatory role played by the poly(ADP-ribosyl)ation process, H1 variants were purified in their native and poly(ADP-ribosyl)ated forms from L929 mouse fibroblasts and compared for their ability to induce the formation of cross-linked polymers when bound to DNA. Our data show that, in H1–DNA complexes, H1e is the

Abbreviations used: MNNG, *N*-methyl-*N'*-nitro-*N*-nitrosoguanidine; DTT, dithiothreitol.

§ To whom correspondence should be addressed.

only H1 histone variant able to allow H1–H1 interactions and promote possible chromatin condensation. This effect is decreased by the poly(ADP-ribosyl)ation of this H1 variant.

MATERIALS AND METHODS

Preparation of native and poly(ADP-ribosyl)ated histone H1

L929 mouse fibroblasts were grown in BHK21 medium with the addition of 10 % (v/v) newborn calf serum in a humidified 5 % CO_2 atmosphere at 37 °C. At a cell density of 20×10^6 cells/175 cm^2 flask, cells were washed with PBS, pH 7.2, removed from flasks by treatment with trypsin and collected by low-speed centrifugation. Cells (7×10^8) were then permeabilized at 4 °C for 30 min in an incubation medium of 10 mM Tris/HCl buffer (pH 7.8) containing 5 mM dithiothreitol (DTT), 4 mM $MgCl_2$ and 1 mM sodium EDTA. To obtain histone H1 enriched in its poly(ADP-ribosyl)ated form [48], cells were incubated for 10 min with 50 μM [^{32}P]NAD$^+$ in 50 mM Tris/HCl buffer (pH 7.8) containing 10 mM $MgCl_2$, 45 mM KCl, 5 mM DTT, 0.1 mM PMSF and 30 μM *N*-methyl-*N'*-nitro-*N*-nitrosoguanidine (MNNG). After precipitation with 20 % (w/v) trichloroacetic acid on ice, cells were washed twice with 5 % (w/v) trichloroacetic acid, twice with ethanol and once with diethyl ether.

Histone H1 was purified from L929 mouse fibroblast cells and from the same poly(ADP-ribosyl)ated cells by extraction overnight in 0.2 M H_2SO_4 and, after centrifugation and dialysis, re-extracted overnight in 10 % (w/v) $HClO_4$ [49].

Separation and analysis of H1 histone variants

H1 histone variants were separated, by the method of Quesada et al. [50], on a reverse-phase RPC4-300 Å column (5 mm × 250 mm; Vydoc) using a Perkin-Elmer 410 Apparatus equipped with a Diode-Array 235 UV detector. The crude H1 preparations were dissolved, for loading on to the column, in 0.1 % (v/v) trifluoroacetic acid in water. Elution was performed at room temperature at a flow rate of 1 ml/min, using a linear gradient (0.1 % trifluoroacetic acid in water to 0.1 % trifluoroacetic acid in 95 % acetonitrile). Protein fractions of 0.5 ml were collected, lyophilized and analysed on SDS/15 %-PAGE. Protein concentrations were determined by densitometric scanning (Bio Image; Millipore) of silver-stained proteins after SDS/PAGE by a commercial adaptation of Bradford's procedure [51] and verified by analysis of their acid hydrolysates (6 M HCl at 110 °C for 24 h) on an LKB 4400 amino acid analyser.

Characterization of poly(ADP-ribosyl)ated histone H1

Histone H1 and its poly(ADP-ribosyl)ated isoform were analysed by SDS/15 %-PAGE. After staining with 0.1 % Coomassie Brilliant Blue R-250 or with silver nitrate, gels were dried on a Bio-Rad gel dryer and autoradiographed using Kodak RX film plates. The amount of poly(ADP-ribose) associated with histone H1 and its somatic variants was estimated by measuring [^{32}P]NAD$^+$-derived radioactivity using a Beckman LS-6800 liquid scintillation spectrometer.

Purification of ADP-ribose polymers from histone H1 and its somatic variants

Histone H1 and its variants (as eluted from the HPLC column) were resuspended in 10 mM Tris/HCl buffer (pH 7.8) containing 1 mM sodium EDTA and processed, by the method of Malanga and Althaus [52], for the purification of protein-bound ADP-ribose polymers. Briefly, proteins were digested overnight with proteinase K (200 μg/ml) at 37 °C. An equal volume of 1 M KOH plus 100 mM sodium EDTA was then added and the incubation was continued for 2 h at 37 °C. After adjusting the pH to a value of 9 by addition of 6 M HCl, the solution was centrifuged at 2300 ***g*** for 10 min at 25 °C. After repeated extraction of the solution with equal volumes of chloroform/3-methylbutan-1-ol (24:1, v/v), ADP-ribose polymers were loaded on a 20 % polyacrylamide gel in 0.09 M Tris/borate buffer, pH 8.3 [53]. The gels were run for 5 h in the same buffer, then dried and autoradiographed on an X-ray film. Poly(ADP-ribose) chain lengths were calculated on the basis of their mobility compared with that of the dyes Bromophenol Blue and Xylene Cyanol [54].

Assay of methyl-accepting ability

Nuclei from L929 mouse fibroblast cells were pelleted by Microfuge centrifugation at 450 ***g*** for 5 min [55]. Crude nuclei pellets were resuspended in 50 mM Tris/HCl buffer (pH 7.8), 45 mM KCl, 20 mM $MgCl_2$ and 5 mM DTT, and incubated at 37 °C for different times. Their methyl-accepting ability was assayed, as described by Caiafa et al. [56], by adding 30–35 μCi/ml *S*-adenosyl-L-[*methyl*-^{3}H]methionine (New England Nuclear; specific radioactivity 70–80 μCi/mmol) as methyl donor and DNA methyltransferase (EC 2.1.1.37), purified from human placenta nuclei as described by Carotti et al. [57].

Crude nuclei were prepared from fibroblasts. When required, they were induced, in parallel, to increase their poly(ADP-ribosyl)ation by exposure to 500 μM [^{32}P]NAD$^+$ [54]. The reaction was stopped by heating at 60 °C for 2 h in the presence of 1 % (w/w) SDS and 0.3 mg/ml proteinase K. After cooling on ice, 70 μg/ml salmon sperm DNA was added to serve as carrier, and DNA was precipitated at 0 °C with 20 % (w/v, final concentration) trichloroacetic acid. The pellets, washed again with 5 % trichloroacetic acid, were resuspended in 0.5 ml of 0.5 M NaOH and heated to 60 °C for 30 min to remove, by alkaline hydrolysis, any contaminating RNA. After cooling, DNA was precipitated with 15 % trichloroacetic acid and then recovered on glass-fibre paper (GF/C; Whatman), repeatedly washed with 5 % trichloroacetic acid and then with 95 % ethanol. The radioactivity was measured in a Beckman LS-6800 liquid scintillation spectrometer.

Preparation of DNA from condensed chromatin

Nuclei from human placenta [58] were digested by *Staphylococcus aureus* nuclease (EC 3.1.31.5; Boehringer) at 3.5 units/mg of DNA for 10 min at 37 °C, digestion being stopped by the addition of ice-cold 5 mM EDTA. Chromatin-bound proteinases were irreversibly inhibited during all preparation steps by 1 mM PMSF (Fluka). Nuclease-sensitive DNA fragments originating from decondensed chromatin were removed by 30 min centrifugation at 12000 ***g*** on a Sorvall centrifuge using the SS34 rotor. The pellet, which contained the condensed chromatin, was resuspended in a Potter–Elvehjem homogenizer and layered on to a linear 5–30 % (w/v) sucrose gradient in 10 mM Tris/HCl (pH 7.5), 1 mM EDTA, 1 mM PMSF, 0.5 mM DTT and 10 % (v/v) glycerol. After 38 h centrifugation at 4 °C in a Beckman L5 ultracentrifuge at 120000 ***g*** (SW-27 rotor), the gradient was fractionated into 35 fractions of 1 ml each, and the oligonucleosomal fractions, characterized by the presence of 6–8 nucleosomes per particle, were dialysed against 1 mM EDTA in 10 mM Tris/HCl (pH 7.5) buffer. The DNA concentration was evaluated from the absorbance at 260 nm. The size of the DNA, estimated by 0.8 % agarose gel electrophoresis, corresponded to 1.2–1.6 kbp.

Formation of H1–DNA complexes

Complexes between each H1 histone somatic variant [in native or poly(ADP-ribosyl)ated form] and DNA were obtained, by the method of Clark and Thomas [30], by mixing a concentrated solution of DNA into a dilute solution of H1 histone in 40 mM NaCl buffered at pH 7.4 with 1 mM sodium phosphate and 0.2 mM EDTA. These samples, prepared at a final DNA concentration of 30 μg/ml and at a H1/DNA ratio of 3:10 (w/w), were incubated for 2 h at room temperature in siliconized Microfuge tubes. For cross-linking experiments, dithiobis(succinimidyl propionate) (Pierce) was added as chemical cross-linking agent from a stock solution in DMSO to a final concentration of 0.2 mg/ml. After 20 min at room temperature, the reaction was stopped by addition of ice-cold trichloroacetic acid to a final concentration of 25% (w/v). The precipitated samples, washed with acetone plus 5 mM HCl and rinsed with pure acetone, were analysed by SDS/7%-polyacrylamide slab gel electrophoresis in 1 mM phosphate buffer, pH 6.6 [59], omitting mercaptoethanol from the sample buffer in order to preserve the cross-links.

RESULTS

Purification and characterization of poly(ADP-ribosyl)ated H1 histone variants

Histone H1 was purified in its poly(ADP-ribosyl)ated form from L929 mouse fibroblasts. Cells were permeabilized and pre-incubated with the alkylating carcinogen MNNG in order to induce nicks on the DNA and to stimulate the poly(ADP-ribosyl)ation process, and with [^{32}P]NAD$^+$ to label the ADP-ribose-containing polymers [52]. Autoradiography showed the covalent association of H1 histone with poly(ADP-ribose) (Figure 1). Since the poly(ADP-ribosyl)ation of H1 histone results in retarded migration of the modified protein on gel electrophoresis compared with the unmodified one, most of the radioactivity appeared higher up the gel than the two sharp bands that are H1 histone variants with a single ADP-ribose attached. The disappearence of radioactivity following digestion of the modified H1 histone with proteinase K showed that all of the radioactivity was associated with this protein (results not shown).

Histone H1 somatic variants enriched in their poly(ADP-ribosyl)ated isoforms were purified by reverse-phase HPLC. Figure 2 shows the elution profile of H1 variants, and this is correlated in the inset with the ADP-ribose-associated radioactivity present in each peak. In terms of specific radioactivity, the highest poly(ADP-ribose) content was in H1a (3500 c.p.m./unit area), followed by H1b (1200 c.p.m./unit area), H1c (900 c.p.m./unit area) and H1e (400 c.p.m./unit area). Figure 3 shows the size distribution of the ADP-ribose polymers associated with the H1b, H1c and H1e variants, as compared

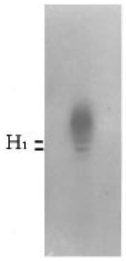

Figure 1 SDS/PAGE analysis of H1 histone enriched in its poly(ADP-ribosyl)ated isoform

An autoradiograph is shown of H1 histone purified from L929 mouse fibroblasts incubated with 50 μM [^{32}P]NAD$^+$.

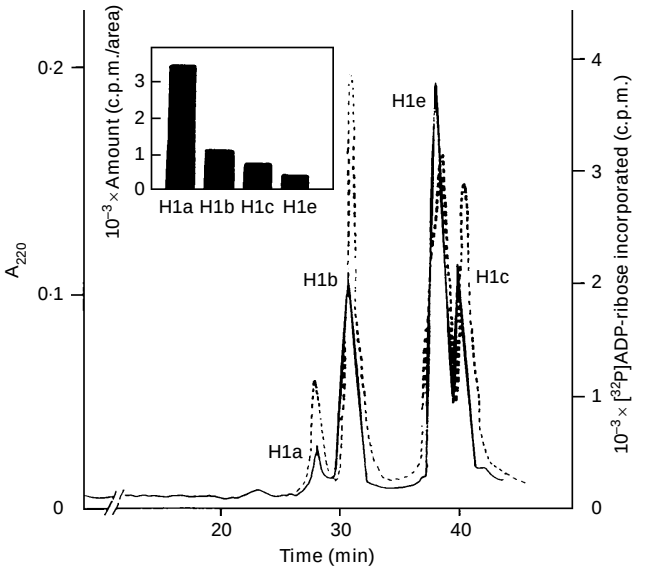

Figure 2 Separation and characterization by reverse-phase HPLC of H1 histone variants enriched in the poly(ADP-ribosyl)ated isoform

The elution profile from the reverse-phase HPLC column is shown: solid line, A_{220}; broken line, ^{32}P-labelled poly(ADP-ribose) incorporated into H1 histone variants. Inset: distribution of labelled ADP-ribose polymers associated with each H1 histone variant.

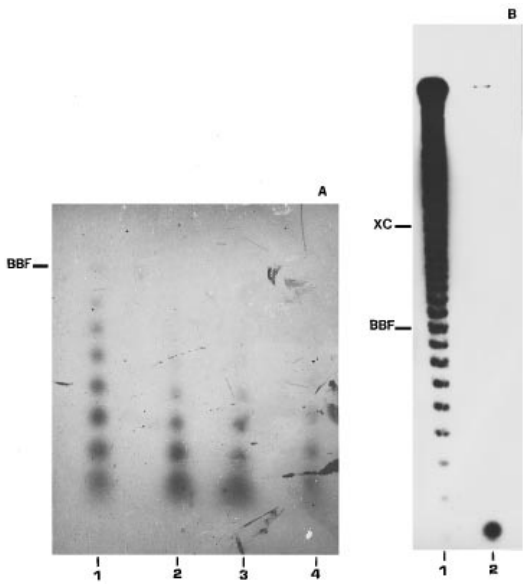

Figure 3 Size distribution of ADP-ribose polymers produced *in vivo*

(**A**) Autoradiography of ADP-ribose polymers extracted from H1 histone purified from L929 mouse fibroblasts (lane 1) and from H1 histone variants H1b, H1e and H1c (lanes 2–4 respectively). Equal amounts of radioactivity were loaded for each variant. (**B**) Autoradiography of total ADP-ribose polymers extracted from L929 mouse fibroblasts (lane 1); lane 2 contains an identical sample digested with snake venom phosphodiesterase, which releases ADP-ribose residues. Markers: BBF, Bromophenol Blue; XC, Xylene Cyanol.

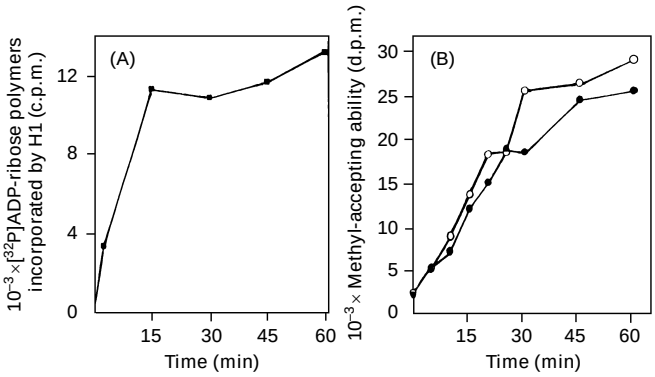

Figure 4 Interactions of H1 histone with linker DNA as assessed by the methyl-accepting ability of native and poly(ADP-ribosyl)ated nuclei

(**A**) Time course of incorporation of [^{32}P]ADP-ribose polymers associated with H1 histone extracted using 10% (w/v) $HClO_4$ from nuclei incubated with 50 μM [^{32}P]NAD^+. (**B**) Methyl-accepting ability of native (●) and poly(ADP-ribosyl)ated (○) nuclei.

with those of total H1 histone (Figure 3A) and with those from the same L929 fibroblasts (Figure 3B).

Modulation of chromatin structure by poly(ADP-ribosyl)ation: does this modification alter the interaction of histone H1 with linker DNA?

Our previous data [39] showed that depletion of H1 from native oligonucleosomes increased the methyl-accepting ability of CpG dinucleotides in linker DNA. Taking into account poly(ADP-ribose)-dependent chromatin decondensation [40–46], we considered the possibility that this modification may alter the interaction of histone H1 with linker DNA, causing a change in the methyl-accepting ability of CpG dinucleotides present essentially in their unmethylated form on linker DNA [61–64]. Our aim was, therefore, to compare the methyl-accepting ability of native nuclei with that of nuclei in which chromatin decondensation was induced by poly(ADP-ribosyl)ation. Figure 4(A) shows the effective incorporation of ADP-ribose polymers into H1 histone during the experimental time. The methyl-accepting ability was not increased (if anything, it was slightly decreased) in the decondensed chromatin structure induced by the poly(ADP-ribosyl)ation process (Figure 4B), suggesting that the poly(ADP-ribosyl)ated H1 histone has not been removed from linker DNA, despite possible alterations in the H1–DNA interactions.

Analysis of H1–H1 interactions in (histone H1 variant)–DNA complexes

The distance between H1 molecules in the complexes between H1 histone somatic variants and DNA purified from condensed chromatin was analysed in terms of their ability to be chemically cross-linked by dithiobis(succinimidyl propionate), a bifunctional amino group reagent able to cross-link, under appropriate conditions, the nucleophilic unprotonated ϵ-amino groups of lysine side chains in proteins [65]. We investigated, under conditions of ionic strength known to promote the condensation of polynucleosomes into chromatin fibres [29], the size distribution of (H1 variant)–(H1 variant) polymers formed upon addition of the bifunctional cross-linking agent at an H1 variant/DNA ratio of 3:10 (w/w). Polymers were separated by

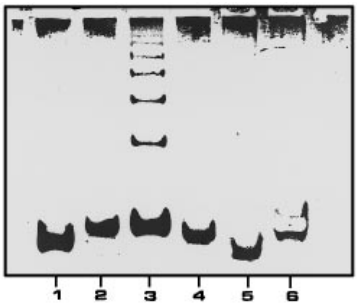

Figure 5 Cross-linking analysis to investigate the role of each H1 histone variant in the formation of H1–H1 polymers

SDS/PAGE patterns are shown of H1 histone variants [at a 3:10 (w/w) H1/DNA ratio] incubated with 1.2 kb oligonucleosomal DNA in 40 mM NaCl for 1 h at room temperature and then treated with dithiobis(succinimidyl propionate) (0.2 mg/ml) for 20 min. H1a, H1b, H1e and H1c are in lanes 1–4 respectively. Untreated histone H1 (lane 5) and histone H1 treated with dithiobis(succinimidyl propionate) (lane 6) were run as controls in the absence of DNA.

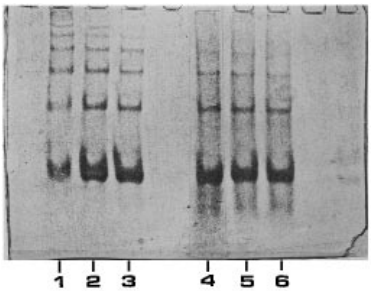

Figure 6 Cross-linking analysis to investigate the effect of poly(ADP-ribosyl)ation of H1e on the formation of H1–H1 polymers

SDS/PAGE patterns are shown of the products of cross-linking of the H1e histone isoforms at different H1/DNA ratios. H1e was incubated with 1.2 kb oligonucleosomal DNA in 40 mM NaCl for 1 h at room temperature and then treated with dithiobis(succinimidyl propionate) (0.2 mg/ml) for 20 min. Lanes 1–3, H1e/DNA at 3:10, 2:10 and 1:10 (w/w) respectively; lanes 4–6, enriched poly(ADP-ribosyl)ated H1e/DNA at 3:10, 2:10 and 1:10 (w/w) respectively.

SDS/7%-PAGE and visualized by silver staining. Among the H1 histone somatic variants, H1e was the only one able to generate dimers, trimers, tetramers, pentamers and even some longer oligomers upon cross-linking; a similar pattern of polymers was absent when the other H1 histone variants were used (Figure 5).

How does poly(ADP-ribosyl)ation modify the cross-linking efficiency of DNA-bound H1e?

Histone H1e and H1e enriched in its poly(ADP-ribosyl)ated isoform were compared at different H1 variant/DNA ratios [1:10, 2:10 and 3:10 (w/w)] for their ability to induce H1–H1 polymers when complexed with DNA. As shown in Figure 6, the poly(ADP-ribosyl)ated variant was less effective in promoting H1–H1 associations.

DISCUSSION

Following on from the model of the 30 nm fibre, put forward by Finch and Klug [10] two decades ago, a variety of other models have been suggested for the structure of chromatin. The first models described a regular structure, termed a solenoid, com-

posed of about six nucleosomes per turn (although according to Walker and co-workers [66,67] this number could be as high as 12) with a fibre thickness of 30 nm and a 10–11 nm pitch for each turn. The solenoid structure requires H1 histone [1–3], although there has been much discussion as to where and how H1 is located in this level of chromatin organization. In the original model [10], H1 histone is proposed to occupy, together with some other non-histone proteins, the central hole of the solenoidal structure. According to the model proposed by McGhee and Felsenfeld [11], H1 histone molecules are alternately located inside and outside the 30 nm fibre. In a further model [13] all H1 histone molecules are present on the inner side of the nucleofilament, with a radial location corresponding to the inner face of the nucleosomes, while according to Leuba et al. [12], H1 histone is accessible to proteolytic enzymes from the external surface of the fibre even in the condensed state. A recent model [47,68,69], obtained using the technique of scanning force microscopy, shows a condensed 30 nm fibre which adopts essentially an irregular, rather than a regular, structure.

Irrespective of a regular or irregular structure of the 30 nm fibre and of the localization of H1 histone in this condensed structure, the presence of H1 histone and the occurrence of H1–H1 interactions are considered to be essential in inducing the formation of and/or in maintaining the condensed chromatin. By using the procedure described by Clark and Thomas [30,32] we found that only H1e histone molecules undergo inter-H1 association when complexed with DNA, while the other somatic variants are present only as monomers. The binding of H1e to DNA allows, therefore, co-operative H1–H1 interactions, indicating a specific role for this variant in promoting high-order chromatin structure.

An interesting approach is to study the processes involved in inducing the ordered decondensation of chromatin structure. Among enzymic post-translational modifications, poly(ADP-ribosyl)ation has been identified as an important factor in altering chromatin structure and, as a consequence, some of its functions. Poly(ADP-ribosyl)ation of H1 histone reportedly acts by 'opening up' the chromatin structure and prevents recondensation of chromatin into higher-order structure [9,40–46]. Although less than 1% of the total H1 histone is poly(ADP-ribosyl)ated [70], this appears to be enough to cause distinct changes in chromatin structure.

Since H1e appears to be the only somatic variant able to stabilize the higher-order structure of chromatin, we examined its poly(ADP-ribosyl)ated isoform to verify whether and how such a modification can convert the condensing role of this histone into a decondensing one. The use of H1e variant preparations enriched in the poly(ADP-ribosyl)ated isoform confirmed this working hypothesis, and suggests a dynamic role in chromatin condensation for this variant which is modulated by this post-synthetic modification. The methyl-accepting ability of linker DNA was not increased by H1 poly(ADP-ribosyl)ation, confirming [9] that H1 histone also remains associated with linker DNA during the poly(ADP-ribosyl)ation-dependent chromatin decondensation process.

In conclusion, irrespective of whether the higher-order folding of the nucleosomal fibre corresponds to a regular helical structure [1–3,10–13] or an irregular three-dimensional array of nucleosomes [47,68,69], the H1e histone variant appears to be critically involved in ensuring the occurrence of the H1–H1 interactions essential for the induction and/or stabilization of the higher-order levels of chromatin organization. Poly(ADP-ribosyl)ation could decrease H1e–H1e interactions and, as a consequence, induce alterations in chromatin structure that would inevitably influence gene expression and possibly other nuclear functions.

This work was supported by the Italian Ministry of University and Scientific and Technological Research (60%, Progetti di Ateneo), by the Fondazione 'Istituto Pasteur-Fondazione Cenci Bolognetti' and by the Associazione Italiana per la Ricerca sul Cancro (A.I.R.C.). We thank Dr. L. Lenti for access to HPLC facilities and R. C. Traversi for technical assistance.

REFERENCES

1 Thoma, F., Koller, T. and Klug, A. (1979) J. Cell Biol. **83**, 403–427
2 Butler, P. J. G. and Thomas, J. O. (1980) J. Mol. Biol. **140**, 505–529
3 Thoma, F. (1988) in Architecture of Eukaryotic Genes (Kahl, G., ed.), pp. 163–185, VCH, Weinheim
4 Boulikas, T., Wiseman, J. M. and Garrard, W. T. (1980) Proc. Natl. Acad. Sci. U.S.A. **77**, 127–131
5 Allan, J., Hartman, P. G., Crane Robinson, C. and Aviles, F. X. (1980) Nature (London) **288**, 675–679
6 Staynov, D. Z. and Crane Robinson, C. (1988) EMBO J. **7**, 3685–3691
7 Allan, J., Mitchell, T., Harbone, N., Bohm, L. and Crane Robinson, C. (1986) J. Mol. Biol. **187**, 591–601
8 Felsenfeld, G. (1992) Nature (London) **355**, 219–224
9 Boulikas, T. (1991) Anticancer Res. **11**, 489–528
10 Finch, J. T. and Klug, A. (1976) Proc. Natl. Acad. Sci. U.S.A. **73**, 1897–1901
11 McGhee, J. D. and Felsenfeld, G. (1980) Annu. Rev. Biochem. **49**, 1115–1156
12 Leuba, S. H., Zlatanova, J. and van Holde, K. (1993) J. Mol. Biol. **229**, 917–929
13 Graziano, V., Gerchman, S. E., Schneider, D. K. and Ramakrishnan, V. (1994) Nature (London) **268**, 351–354
14 Izaurralde, E., Kas, E. and Laemmli, U. K. (1989) J. Mol. Biol. **210**, 573–585
15 Cole, K. D. (1987) Int. J. Peptide Protein Res. **30**, 433–449
16 Pehrson, J. R. and Cole, R. D. (1982) Biochemistry **21**, 456–460
17 Lennox, R. W. and Cohen, L. H. (1983) J. Biol. Chem. **258**, 262–268
18 Lennox, R. W. (1984) J. Biol. Chem. **259**, 669–672
19 Giancotti, V., Bandiera, A., Ciani, L., Santoro, D., Crane Robinson, C., Goodwin, G. H., Biocchi, M., Dolcetti, R. and Casetta, B. (1993) Eur. J. Biochem. **213**, 825–832
20 Huang, H.-C. and Cole, R. D. (1984) J. Biol. Chem. **259**, 14237–14242
21 Baubichon-Cortay, H., Mallet, L., Denoroy, L. and Roux, B. (1992) Biochim. Biophys. Acta **1122**, 167–171
22 Schulze, E., Trieschmann, L., Schulze, B., Schmidt, E. R., Pitzel, S., Zechel, K. and Grossbach, U. (1993) Proc. Natl. Acad. Sci. U.S.A. **90**, 2481–2485
23 Liao, L. W. L. and Cole, R. D. (1981) J. Biol. Chem. **254**, 6751–6755
24 Liao, L. W. L. and Cole, R. D. (1981) J. Biol. Chem. **256**, 10124–10128
25 Liao, L. W. L. and Cole, R. D. (1981) J. Biol Chem. **256**, 11145–11150
26 De Lucia, F., Faraone Mennella, M. R., D'Erme, M., Quesada, P., Caiafa, P. and Farina, B. (1994) Biochem. Biophys. Res. Commun. **198**, 32–39
27 Santoro, R., D'Erme, M., Mastrantonio, S., Reale, A., Marenzi, S., Saluz, H. P., Strom, R. and Caiafa, P. (1995) Biochem. J. **305**, 739–744
28 Johnson, C. A., Goddard, J. P. and Adams, R. L. P. (1995) Biochem. J. **305**, 791–796
29 Widom, J. (1986) J. Mol. Biol. **190**, 411–424
30 Clark, D. J. and Thomas, J. O. (1986) J. Mol. Biol. **187**, 569–580
31 De Bernardin, W., Losa, R. and Koller, T. (1986) J. Mol. Biol. **189**, 503–517
32 Clark, D. J. and Thomas, J. O. (1988) Eur. J. Biochem. **178**, 225–233
33 Wu, R. S., Panusz, H. T., Hatch, C. L. and Bonner, W. M. (1986) CRC Crit. Rev. Biochem. **20**, 201–263
34 Zlatanova, J. (1990) Trends Biochem. Sci. **15**, 273–276
35 Tazi, J. and Bird, A. (1990) Cell **60**, 909–920
36 Kamakaka, R T. and Thomas, J. O. (1990) EMBO J. **9**, 3997–4006
37 Jost, J. P. and Hofsteenge, J. (1992) Proc. Natl. Acad. Sci. U.S.A. **89**, 9499–9503
38 Laybourn, P. J. and Kadonaga, J. T. (1991) Science **254**, 238–245
39 D'Erme, M., Santoro, R., Allegra, P., Reale, A., Strom, R. and Caiafa, P. (1993) Biochim. Biophys. Acta **1173**, 209–216
40 Poirier, G. G., De Murcia, G., Jongstra-Bilen, J., Niedergang, C. and Mandel, P. (1982) Proc. Natl. Acad, Sci. U.S.A. **79**, 3423–3427
41 Aubin, R. J., Fréchette, A., de Murcia, G., Mandel, P., Grodin, G. and Poirier, G. G. (1983) EMBO J. **2**, 1685–1693
42 De Murcia, G., Hulersky, A., Lamarre, D., Gaudreau, A., Pouyet, J., Daune, M. and Poirier, G. G. (1986) J. Biol. Chem. **261**, 7011–7017
43 De Murcia, G., Huletsky, A. and Poirier, G. G. (1988) Biochem. Cell Biol. **66**, 626–635
44 Huletsky, A., de Murcia, G., Muller, S., Hengartner, M., Ménard, L., Lamarre, D. and Poirier, G. (1989) J. Biol. Chem. **264**, 8878–8885
45 Burzio, L. O., Riquelme, P. T. and Koide, S. S. (1979) J. Biol. Chem. **254**, 3029–3037
46 Ogata, N., Ueda, K., Kawaiki, M. and Hayashi, O. (1981) J. Biol. Chem. **256**, 4135–4137

47 Leuba, S. H., Yang, G., Robert, C., Samori, B., van Holde, K., Zlatanova, J. and Bustamante, C. (1994) Proc. Natl. Acad. Sci. U.S.A. **91**, 11621–11625
48 Adamietz, P.and Bredehorst, R. (1978) Eur. J. Biochem. **91**, 317–326
49 Johns, E.W (1977) Methods Cell Biol. **16,** 183–203
50 Quesada, P., Farina, B. and Jones, R. (1989) Biochim. Biophys. Acta **1007**, 167–175
51 Bradford, M. M. (1976) Anal. Biochem. **72**, 248–254
52 Malanga, M. and Althaus, F. R. (1994) J. Biol. Chem. **269**, 17691–17696
53 Panzeter, P. L., Realini, C. A. and Althaus, F. R. (1992) Biochemistry **31**, 1379–1385
54 Alvarez-Gonzalez, R. and Jacobson, M. K. (1987) Biochemistry **26**, 3218–3222
55 Davis, T., Rinaldi, A., Clark, L. and Adams, R. L. P. (1986) Biochim. Biophys. Acta **866**, 233–241
56 Caiafa, P., Mastrantonio, S., Attinà, M., Rispoli, M. and Strom, R. (1988) Biochim. Biophys. Acta **951**, 191–200
57 Carotti, D., Palitti, F., Mastrantonio, S., Rispoli, M., Strom, R., Amato, A., Campagnari, F. and Whitehead, E. P. (1986) Biochim. Biophys. Acta **866**, 135–143
58 Rickwood, D. and Birnie, G. D. (1986) in Subnuclear Components (Birnie, G. D., ed.), pp. 129–186, Butterworths, London and Boston
59 Thomas, J. O. and Kornberg, R. D. (1978) Methods Cell Biol. **18**, 429–440
60 Reference deleted
61 Razin, A. and Cedar, H. (1977) Proc. Natl. Acad. Sci. U.S.A. **74**, 2725–2728
62 Solage, A. and Cedar, H. (1978) Biochemistry **17**, 2934–2938
63 Adams, R. P. L., David, T., Fulton, J., Kirk, D., Qureshi, M. and Burdon, R. H. (1984) Curr. Top. Microbiol. Immunol. **108**, 143–156
64 Caiafa, P., Attinà, M., Cacace, F., Tomassetti, A. and Strom, R. (1986) Biochim. Biophys. Acta **867**, 195–200
65 Lomant, A. J. and Fairbanks, G. (1976) J. Mol. Biol. **104**, 243–261
66 Walker, P. R., Sikorska, M. and Whitfield, J. F. (1986) J. Biol. Chem. **261**, 7044–7051
67 Walker, P. R. and Sikorska, M. (1987) J. Biol. Chem. **262**, 12223–12227
68 Zlatanova, J., Leuba, S. H., Yang, G., Bustamante, C., and van Holde, K. (1994) Proc. Natl. Acad. Sci. U.S.A. **91**, 5277–5280
69 van Holde, K. and Zlatanova, J. (1995) J. Biol. Chem. **270**, 8373–8376
70 Braeuer, H. C., Adamietz, P., Nellessen, U. and Hilz, H. (1981) Eur. J. Biochem. **114**, 63–68

Received 8 November 1995/29 January 1996; accepted 31 January 1996